

Gamma Radiation Shielding Performance of Cement–Bambusa Vulgaris Mortar Composites

Lateef O. Mustapha^{1*}, Ibrahim W. Fawole², Ilesanmi A. Ojo¹, Ganiu A. Tikarewa³, Abdullahi U. U. Ocheni², Morenkeji W. Atanda¹ and Peter O. Egbayelo¹

¹Department of Physical Sciences, Al-Hikmah University, Ilorin, Kwara State, Nigeria

²Department of Physics, University of Maiduguri, Maiduguri, Borno State, Nigeria

³Department of Mechanical Engineering, Obafemi Awolowo University, Ile-Ife, Osun State, Nigeria

*Corresponding author: muslaty2k@gmail.com

Abstract

Lead and concrete blocks are well known for shielding against ionizing radiation, but their use is limited due to their high density, toxicity, and environmental concerns. This study investigates the potential of *Bambusa vulgaris* (bamboo powder)-based mortar composites as an alternative gamma-ray radiation-shielding material. Different blends of bamboo powder, sand, and cement were chemically treated to produce binary and ternary composites. The elemental composition of *Bambusa vulgaris* was determined using X-ray fluorescence (XRF), while the radiation attenuation coefficients of the samples against rays were determined using a NaI(Tl) scintillation detector and Cs-137 gamma source (662 keV). Key shielding parameters, including Linear and Mass Attenuation Coefficients (LACs and MACs), Half-Value Layer (HVL), Tenth-Value Layers (TVLs), Mean Free Paths (MFPs), and compressive stress, were determined. The composite containing 57.14% bamboo, 28.57% sand, and 14.29% cement exhibited the most superior attenuation properties with LAC, MAC, HVL, TVL, MFP, and stress of 1.015 cm⁻¹, 1.067 cm²/g, 0.683 cm, 2.269 cm, 0.985 cm, and 0.620 kPa, respectively. The composite exhibits radiation attenuation capability but a lower mechanical strength. Thus, bamboo-based mortar may be explored for applications requiring gamma radiation protection.

Article Info.

Keywords:

Bamboo, Gamma Radiation, Mortar, Attenuation, Shielding.

Article history:

Received: Dec. 25, 2025

Revised: Feb. 24, 2026

Accepted: Mar. 09, 2026

Published: Jun. 01, 2026

1. Introduction

The discovery and application of ionising radiation have had a profound impact on both physics and medicine. Among the various forms of ionising radiation, gamma rays possess the highest penetrating power and deposit high energy within biological tissues. This interaction can damage cellular structures and DNA, resulting in both immediate and long-term health risks, including cancer. Consequently, gamma radiation has been classified as carcinogenic by the World Health Organization WHO [1] and the International Agency for Research on Cancer (IARC) [2], due to its capacity to induce oxidative stress and DNA strand breaks. As a result, effective shielding is essential in nuclear, industrial, and medical environments that use gamma radiation.

Traditionally, gamma shielding has relied on high-density materials [3, 4], with concrete [5, 6] and lead [7, 8] being most commonly employed. Concrete is widely used because of its non-toxicity, availability, relatively low cost, ease of production, and flexibility in fabricating desired geometrical shapes. However, due to its moderate density (approximately 2.0-3.0 g/m³), concrete often requires thick, bulky structures to achieve adequate radiation protection, thereby increasing construction costs and limiting its use in space-constrained environments [9]. Lead, on the other hand, offers superior attenuation efficiency due to its high atomic number and density. Despite these advantages, lead poses serious concerns regarding toxicity [10] and environmental contamination [11], which limit its large-scale and long-term application, especially in medical and residential settings. These limitations have driven



growing interest in developing lead-free radiation shielding materials that are not only effective but also lightweight, sustainable, and environmentally friendly [3, 12]. In recent years, research efforts have focused on optimizing conventional shielding materials by incorporating alternative aggregates and fillers that can improve attenuation performance while reducing environmental impact and costs. In response to this challenge and as a way of amelioration, several studies have explored the use of natural and industrial by-products as partial or complete substitutes for conventional aggregates in shielding composites. Materials such as clay minerals [13], fly ash [14], agricultural by-products, rice husk ash [15], palm oil fuel ash [16, 17], and sawdust [17] have shown remarkable properties and thus attracted researchers interest. This is ascribed to their availability, sustainability and attenuation potential. To a greater degree, the use of these materials as cement-based matrices may accelerate waste recycling process and viable construction practices.

Bambusa vulgaris, a common bamboo, was adopted for radiation shielding. It has a wide distribution across the continents of Africa, Asia, and Latin America, with a rapid growth rate to maturity of 3 to 5 years [18, 19]. It is a highly renewable, regenerative resource, a sustainable material with favourable mechanical properties, combining high tensile and compressive strength with low density and good durability. *Bambusa vulgaris* has a chemical composition of cellulose (60 - 70 %) and lignin (10 - 20 %), while its ash powder is notable for its silica content, which ranges from 9-12 % [20]. The coexistence of carbon-based constituents and silica in bamboo species provides mechanical support and enhances radiation shielding. Prior studies [21, 22] on *Bambusa vulgaris* as fibres and particles in construction and composite materials, particularly for structural panels, reinforced concrete, and lightweight building materials, aimed to enhance mechanical strength, durability, and thermal insulation in the host. The application of *Bambusa vulgaris* composite for gamma shielding, despite extensive studies, has received less attention. Most available shielding materials still involve trade-offs between attenuation efficiency, mechanical strength, cost, environmental impact, and ease of fabrication. This has elicited a desire to develop substitute materials that meet the structural and shielding capabilities and can perform efficiently. The proposed shielding materials should be eco-friendly as well as lightweight, but still integrate mechanical characteristics with efficient gamma attenuation that meet medical and industrial standards.

In this work, *Bambusa vulgaris* powder was used as a fractional component in mortar composites to provide lightweight, environmentally friendly alternatives for gamma radiation shields. The performance of bamboo–mortar composites as gamma shielding materials was evaluated and compared with that of concrete products.

The bamboo powder was chemically treated using an alkali process, followed by mechanical grinding to improve composite suitability. Gamma attenuation measurements were carried out using a Cs-137 source and a NaI(Tl) scintillation detector. X-ray fluorescence (XRF) analysis was used to characterise the bamboo-based shields. The shielding parameters, linear and mass attenuation coefficients, half-value layer, tenth-value layer, and mean free path, were determined. The mechanical strength of *Bambusa vulgaris* powder as a composite in mortar blocks for gamma shielding was also determined.

2. Materials and Methods

2.1 Samples Preparation

The materials used in this study included Portland cement, clean river sand, pulverised *Bambusa vulgaris* powder as a partial fine aggregate replacement, and potable water. The bamboo powder was obtained from mature *Bambusa vulgaris* culms harvested within the construction site at Al-Hikmah University, Ilorin, Kwara State, Nigeria (Fig. 1a). After harvesting, the culms were air-dried and then immersed in a 1% of sodium hydroxide (NaOH) for 24 hours. The mild alkali treatment, adapted with slight modification from the method reported by Ayoola et al. [21], was carried out to remove surface impurities and improve

interfacial bonds within the cementitious matrix (Fig. 1b). For effective treatment, the bamboos were washed with distilled water to remove alkali residuals, and thereafter sun-dried for three consecutive days to achieve constant weight. To obtain a fine powder less than 4.75 mm, the dried culms were sliced into smaller pieces, milled (Fig. 1b) and sieved with an automatic sieve shaker (ASTM sieve sizes No. 4–200). This is to enable better packing, uniform dispersion within the mortar matrix, and improved interfacial bonding, which, in turn, improves the mechanical performance for effective gamma-radiation shielding (Fig. 1c). A constant water-to-binder ratio of 0.50 was used for the separate preparation of the control and modified mortar specimens. To assess the binary and ternary composites on the physical and mechanical characteristics, in addition to their potential shielding performance, five different mix designs (samples A – E) were developed by varying the proportions of cement, sand, and bamboo powder, as indicated in Table 1. The control mixture (sample A), the well-known conventional mortar, has a proportion of 20 wt.% cement and 80 wt.% sand. The high sand content contributes to density and compressive strength, while cement ensures adequate cohesion. Sample B represents the organic material with a lightweight composite mixture of 20 wt.% cement and 80 wt.% bamboo powder. The absence of sand in this formulation reduces the density and might also limit its mechanical strength and shielding capability. Sample C serves as a hybrid system, designed to balance the mechanical strength with reduced weight. To improve matrix bonding, the cement content was slightly increased to 25 wt.%, with 37.5 wt.% sand and 37.5 wt.% bamboo powder. Due to its lightweight, cost-effective, and eco-friendly nature, bamboo was made the dominant component in sample D with 14.29 wt.% cement, 28.57 wt.% sand, and 57.14 wt.% bamboo powder. In this sample, the low percentage of cement and sand content may reduce compressive strength and durability. To assess the compromise between structural integrity and weight reduction, sample E (20 wt.% cement, 30 wt.% sand, and 50 wt.% bamboo powder) serves as a transitional formulation between samples C and D.



Figure 1: (a) Bamboo sticks before cutting into smaller pieces, (b) Bamboo pieces after treatment with NaOH, (c) Pulverised Bamboo, and (d) Mortar Samples.

Table 1: Five composite sample designations (A–E) with varying proportions of cement, sand, and bamboo powder (in wt.%).

S/N	Designation	Composition
1	A	20.0 (wt.%) cement, 80.0 (wt.%) sand
2	B	20.0 (wt.%) cement, 80.0 (wt.%) bamboo
3	C	25.00 (wt.%) cement, 37.50 (wt.%) sand, 37.50 (wt.%) bamboo
4	D	14.29 (wt.%) cement, 28.57 (wt.%) sand, 57.14 (wt.%) bamboo
5	E	20.0 (wt.%) cement, 30.0 (wt.%) sand, 50.0 (wt.%) bamboo

These mixtures were homogenised mechanically using hand towels and placed into moulds of dimensions $4 \times 4 \times 6$ inches, as shown in Fig. 1d. The specimens were sun-dried for 28 days to allow curing and stabilisation of the cementitious matrix under ambient outdoor conditions (average temperature: 28 - 35 °C; relative humidity: 60 - 80%) in a well-ventilated sheltered area until constant mass was achieved. With a moderately fractional cement component, there is a possibility of a more stable matrix than sample D, while still maintaining lightweight characteristics.

2.2 Characterisation

The experimental methodology involved the investigation of both compositional and radiological shielding parameters. Elemental composition of the bamboo powder was investigated with a Shimadzu EDXRF-702HS X-Ray Fluorescence (XRF) spectrometer at an operating potential and current of 40 kV and 18 mA, respectively, and a counting time of 100 s at the National Institute of Radiation Protection and Research (NIRPR), University of Ibadan, Ibadan. To minimise matrix effects, the samples were fused with lithium tetraborate before analysis, and the major oxides in the bamboo samples, including K_2O , CaO , and MgO , were quantified.

Gamma-ray attenuation measurements were performed using a calibrated Gamma Ray Spectrometer (GRS), shown in Fig. 2a, equipped with a NaI(Tl) scintillation detector; the sample was positioned perpendicular to the beam path, and the NaI(Tl) scintillation detector was aligned along the source–detector axis. The samples, at a distance of 1.50 m from the NaI (Tl) scintillation detector, were irradiated with a Cs-137 gamma source for the photon attenuation test. The Cs-137 source emits monoenergetic gamma photons of 662 keV following beta decay to Ba-137m with a half-life of approximately 30.17 years. The Cs-137 source was securely housed in a lead-shielded container fitted with a narrow collimator to produce a well-defined and focused gamma beam. The experimental geometry was maintained under narrow-beam transmission conditions to minimise scattered radiation effects. The experimental methodology involved investigating both compositional and radiological shielding parameters.

For each sample, the incident (I_0) and transmitted (I) intensities of the gamma beam were recorded. The Linear Attenuation Coefficient (LAC, μ) was calculated using Beer-Lambert's law as shown in Eq. (1):

$$I = I_0 e^{-\mu x} \quad (1)$$

where x is the sample thickness, and μ is the linear attenuation coefficient.

The thickness of a sample required to reduce the intensity of the gamma beam by 50% is the half-value layer (HVL) and was computed using Eq. (2). The thickness of a sample required to reduce the intensity of the incident gamma beam to one-tenth its original value is the tenth-value layer (TVL), which was computed using Eq. (3). Finally, the Mean Free Path (MFP), the distance between successive photon interactions, was computed using Eq. (4):

$$\text{HVL} = \frac{\ln 2}{\mu} \quad (2)$$

$$\text{TVL} = \frac{\ln 10}{\mu} \quad (3)$$

$$\text{MFP} = \frac{1}{\mu} \quad (4)$$

The compressive stress (s) (compressive strength at failure) of each sample was determined using an intelligent pressure meter (OK HARD, 2000 KN), compression testing machine, at the Department of Building, Obafemi Awolowo University, Ile-Ife. This was done by loading each specimen to failure and reporting the peak load divided by the specimen's cross-sectional area.

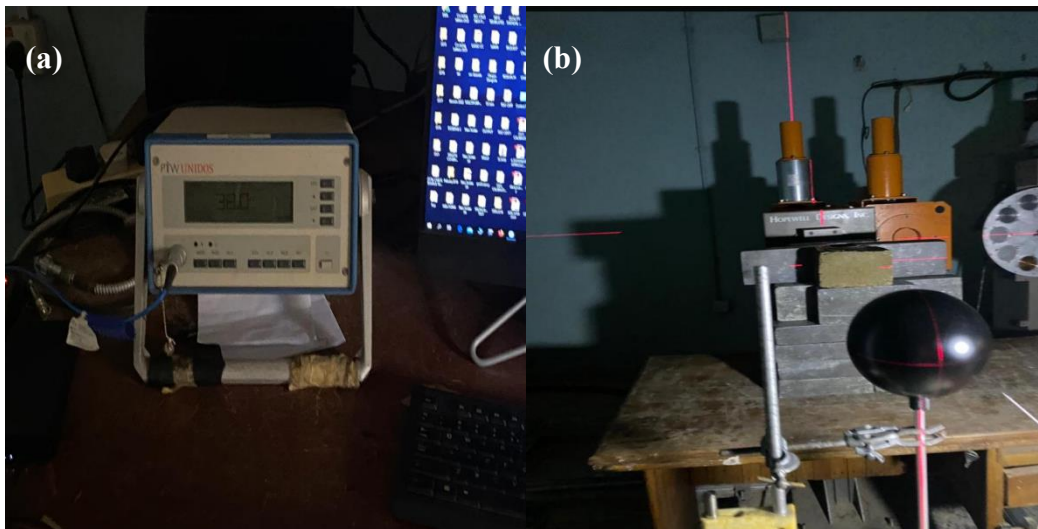


Figure 2: Experimental setup for gamma-ray attenuation measurements: (a) Digital radiation survey meter used for monitoring radiation levels, (b) Narrow-beam transmission geometry showing the collimated Cesium-137 source mounted in a lead-shielded holder, sample positioned perpendicular to the beam path, and NaI(Tl) scintillation detector aligned along the source-detector axis.

3. Results and Discussion

3.1 X-Ray Fluorescence (XRF) Analysis

Various macromineral and micromineral elements were detected in the bamboo sample analyzed with XRF spectrometry. The results of the XRF analysis, shown in Table 2, confirmed that bamboo contains high concentrations of medium-Z oxides, including K_2O (22.76%), CaO (12.17%), MgO (5.23%), alongside other oxides, such as Al_2O_3 , Fe_2O_3 , and P_2O_5 , which were found in moderate amounts. These oxides enhance interactions between photons and matter, and thus directly contribute to the attenuation performance of the bamboo mortar.

Elements, such as potassium ($Z = 19$) and calcium ($Z = 20$), enhance photoelectric and Compton interactions, while magnesium ($Z = 12$) and iron oxides increase the effective electron density of the mortar composites. The presence of oxides in the mortar composites contributes remarkably to the intrinsic organic properties of bamboo and reduces the bulk density. This aids its potential to absorb radiation that surpasses expectations for biomass-based materials. The findings of this study agree with a comparable report [25] that showed composites containing medium-Z oxides to have superior radiation attenuation prospects as compared to fully organic matrices.

Table 2: Result of Analysis Showing the Sample Composition.

S/N	Basic oxides	Formular	Composition%
1	Silicon Oxide	SiO ₂	46.78
2	Aluminium Oxide	Al ₂ O ₃	3.16
3	Magnesium Oxide	MgO	5.23
4	Calcium Oxide	CaO	12.17
5	Iron Oxide	Fe ₂ O ₃	3.28
6	Potassium Oxide	K ₂ O	22.76
7	Sodium Oxide	Na ₂ O	1.18
8	Phosphorus Oxide	P ₂ O ₅	3.52
9	Titanium Oxide	TiO ₂	0.16
10	Manganese Oxide	MnO	1.21
11	Zinc Oxide	ZnO	0.15
12	Copper Oxide	CuO	0.02
13	Sulphide	SO ₃	0.33
14	Chromium Oxide	Cr ₂ O ₅	0.05
15	Loss of Ignition	LOI	3.74

3.2 Radiation Shielding and Mechanical Properties

The values of linear attenuation coefficient (LAC) (μ), mass attenuation coefficient (MAC) (μ_m), HVL, TVL, and mean free paths (MFP) of any material are the most vital indicators of the radiation absorption property of a shielding material over a wide range of energies. Their values highlight how efficient a material is as a radiation absorber. It is clear from Table 3 that as the bamboo powder content varies in the mortar samples, the values of HVL, TVL, and MFP also change appreciably. This highlights the likelihood of gamma-photon interactions in the mortar samples, with particular levels of bamboo replacement leading to fewer photon transmissions. Therefore, these parameters highlight the mortar composites' ability to degrade photon energy efficiently, even at comparatively thin thicknesses.

The radiation shielding properties and mechanical stress of *Bambusa vulgaris* composite mortars were determined, as shown in Table 3. Fig. 2 shows a clear trend in the gamma-ray attenuation parameters for each sample. The linear attenuation coefficient (LAC) increased with bamboo content, particularly for sample D, where the highest value of 1.015 cm⁻¹ was obtained. This value represents an increase of more than 100% when compared to the control sample (sample A), which exhibited an LAC of 0.466 cm⁻¹. The improvement in LAC value suggests that the bamboo powder composite enhances gamma photon attenuation within its matrix. Furthermore, the inclusion of bamboo powder creates a heterogeneous, porous microstructure, increasing the effective photon path length, enhancing the likelihood of multiple scattering events within the composite, promoting greater energy dissipation and absorption, and thus increasing attenuation. The structural arrangement promotes more photon-matter interactions than the homogeneous matrix. Additionally, the porous, particle-graded nature of the composite facilitates Compton scattering, thereby contributing significantly to

attenuation at 662 keV. Multiple scattering within the bamboo-enriched matrix increases photon energy dissipation, reducing transmitted intensity. A comparison of the LAC values across all samples suggests that sample D is the most effective radiation-shielding material, with the highest attenuation, while sample A demonstrates the lowest attenuation. Samples C and E displayed intermediate LACs, and this suggests that the hybrid cement–sand–bamboo composites provide a reasonable compromise between radiation shielding capability and material composition.

Table 3: Linear attenuation coefficient (LAC), mass attenuation coefficient (MAC), HVL, TVL, and mean free path (MFP) for the different samples.

S/N	Samples	LAC (cm ⁻¹)	MAC (cm ² /g)	HVL (cm)	TVL (cm)	MFP (cm)	Stress (kPa)
1	A	0.466	0.233	1.487	4.942	2.146	7000
2	B	0.493	0.499	1.406	4.671	2.028	1400
3	C	0.647	0.460	1.071	3.560	1.546	0.159
4	D	1.015	1.067	0.683	2.269	0.985	0.652
5	E	0.774	0.489	0.895	2.975	1.292	1100

However, the mechanical assessment of the mortar samples highlights a different trend. Sample A exhibited the highest compressive stress resistance of 7000 kPa, indicating the structural robustness of traditional sand-rich mortar. In contrast, sample C showed the least stress resistance (0.159 kPa), emphasising the weak influence of high bamboo content on the mechanical properties of mortar composites. The mechanical strength of mortar composites containing bamboo powder in high proportion is lower than that of the control structural materials. These formulations remain appropriate for non-load-bearing radiation shielding applications, with intermediate compositions offering a balance between attenuation performance and mechanical stability.

Although the addition of bamboo decreases the bulk density of the mortar composites, the presence of medium-Z oxides and the resulting higher effective electron density and internal scattering sites offset this decrease, thereby boosting interactions between photons and the mortar matrix and increasing LAC values. The apparent variation in the mechanical strengths of the mortar samples is due to the differences in the formulations of the mortar composites. Samples containing higher cement and sand proportions, such as sample A, have higher compressive strength as a result of a denser matrix and greater interparticle bonding. Conversely, samples containing higher bamboo powder, particularly sample D, showed a decrease in compressive strength because the organic bamboo particles reduced matrix cohesion, thereby increasing porosity in the mortar samples. These findings demonstrate the essential trade-off between radiation-absorption capability and mechanical performance of the mortar sample, indicating that mortar composite formulation must be made according to specific application requirements.

In contrast, sample A, with limited absorption prospects of radiation, provides outstanding structural stability, making it a choice material for traditional load-bearing applications. Sample E provides a middle ground, combining reasonable radiation absorption capability with average mechanical strength. Generally, these findings show that by carefully adjusting the proportions of bamboo, cement, and sand, composites can be tailored to specific structural applications, such as radiation absorption, panels to lightweight, sustainable structural materials.

The changes in HVL, TVL, and MFP for bamboo composite mortar samples are illustrated in Fig. 3(a, b). These figures show that with the decrease in bamboo content, the HVL, TVL, and MFP decrease; this suggests that bamboo content influences gamma shielding efficiency. Sample A, without bamboo content, shows the highest HVL, TVL, and MFP values. It is evident that variations in the bamboo proportion led to appreciable changes in the values of the HVL, TVL, and mean free path (MFP) of the composites. These changes reflect corresponding variations in the probability of gamma photon interactions with the constituent atoms of the mortar samples, resulting in enhanced attenuation at specific bamboo replacement levels and reduced photon transmission. Furthermore, *Bambusa vulgaris* composite contributes to the enhanced linear attenuation coefficients, HVL of mortar samples reduced from 0.683 to 1.406 cm and from 2.269 to 4.671 cm for TVL according to the bamboo content in the mortar samples, in comparison to the control values of 1.487 cm and 4.942 cm for HVL and TVL, respectively. Also, the decrease in the LAC and MAC values observed for the mortar composites indicates that the dominant photon interaction mechanisms responsible for photon attenuation are the photoelectric effect and Compton scattering [22]. The increased bamboo powder ratios in the mortar mixes caused energy attenuation due to the presence of medium-Z oxides CaO and K₂O in appreciable quantities of 12.17% and 22.76%, respectively, as presented in Table 2. This greatly affected the gamma absorption capability of the mortar samples. The mean free path (MFP) of the mortar mixes decreased the distance between two successive photon interactions as the content of bamboo powder increased. Furthermore, the relationship between LAC and the corresponding compressive stress for the different mortar samples is depicted in Fig. 3(c), drawn with LAC and stress on the left and right side, respectively.

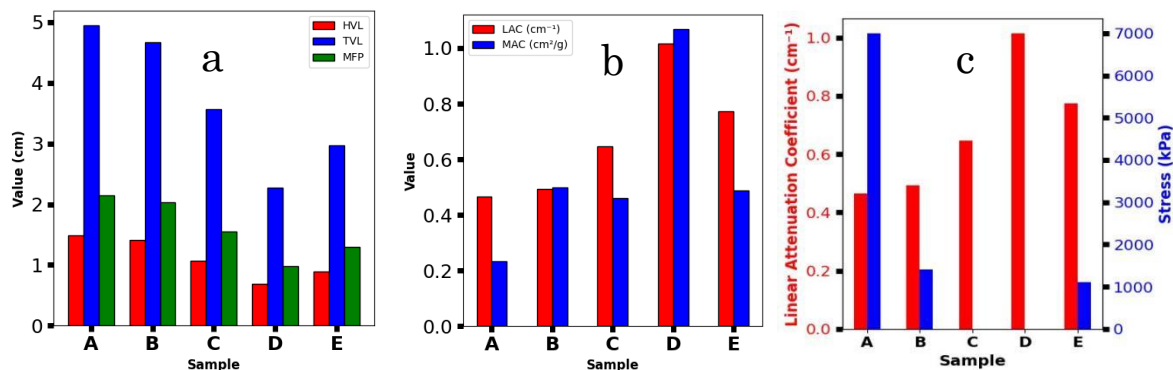


Figure 3: (a) HVL, TVL, and mean free path (MFP) as a function of bamboo composite in mortar samples, (b) variation of linear attenuation coefficient (LAC) and mass attenuation coefficient (MAC) with samples, (c) comparative plot of LAC (left axis) and compressive stress (right axis) showing the relationship between photon shielding efficiency and mechanical strength of the developed composites.

3.3. Comparison with Conventional Materials

Lead remains one of the most efficient shielding materials, with a LAC of $\sim 1.12 \text{ cm}^{-1}$ at 662 keV [23], owing to its high atomic number ($Z = 82$), which strongly favours photoelectric interactions. However, its weight, toxicity, and impact on the environment require safer alternatives [3, 4]. Bamboo mortar composites have potential as an immediate material between lead and conventional concrete. At comparable thickness, the shielding effectiveness of bamboo mortar composites is lower than that of lead but superior to that of conventional cement-based mortars, thereby serving as a potential balance between radiation absorption, sustainability, and material safety. The data in Table 4 further lend credence to the prospect of bamboo-based mortar composites over traditional cement-based mortar for degrading gamma photons at the same energy. These mortars are potential replacements in locations such as

laboratories, medical facilities, temporary shelters, and shielding applications, where low-to-medium-radiation shielding, due to their lower density, renewable features, and reduced environmental impact, is required, along with portability. Table 4 highlights the absorption coefficients of some shielding materials existing in the literature. The assessment of both Tables 3 and 4 reveals that bamboo-based mortar composites have better gamma radiation absorption than ordinary Portland cement mortar composites at the same energy, thus confirming their suitability as a sustainable radiation shield.

Table 4: LAC values of some concrete composites in the literature at 662 keV

S/N	Materials	LAC (cm ⁻¹)	Reference
1	Ordinary Portland concrete	0.151	[23]
2	Portland concrete	0.179	[24]
3	Concrete containing steel mill scale	0.282	[25]
4	Magnetite concrete	0.202	[26]
5	OPC Concrete	0.318	[27]

4. Conclusions

The gamma shielding performance of cement–*Bambusa vulgaris* composite mortar was evaluated using a Cs-137 gamma source with an energy of 662 keV. Linear and mass attenuation coefficients, HVL, TVL, and MFP, were estimated and analysed. Our findings show that adding bamboo powder to mortar improves its ability to attenuate gamma radiation. In particular, composites with higher bamboo content exhibited increased mass attenuation coefficients and corresponding reductions in HVL, TVL, and MFP, indicating better photon absorption capacity. Sample D, with 57.14 wt.% bamboo powder, showed the best attenuation performance of all the samples. For the same radiation attenuation level, a 0.5 cm equivalent thickness of lead would be required to achieve the same result attained by sample D in the current study. Despite the radiation attenuation performance of bamboo powder mortar composites, they exhibited lower mechanical strengths; this may limit their use in load-bearing structures while maintaining radiation shielding efficiency. In addition, optimizing the particle size distribution of bamboo powder and sand, treating the mortar composites in alkali environments, and adjusting the composite density may further improve both the mechanical and radiation attenuation properties of the mortar composites.

Conflict of interest

The authors declare that they have no conflict of interest.

References

1. WHO, *Cytogenetic dosimetry: applications in preparedness for and response to radiation emergencies*. 2011, International Atomic Energy Agency, Department of Nuclear Safety and Security, Incident and Emergency Centre, Vienna.
2. D. Loomis, W. Huang, and G. Chen, The International Agency for Research on Cancer (IARC) evaluation of the carcinogenicity of outdoor air pollution: focus on China. *Chinese J cancer*. **33**(4),189(2014), <https://doi.org/10.5732/cjc.014.10028>
3. N. J. AbuAlRoos, N. A. B. Amin, and R. Zainon, Conventional and new lead-free radiation shielding materials for radiation protection in nuclear medicine: A review. *Radiation Physics and Chemistry*. **165**,108439(2019), <https://doi.org/10.1016/j.radphyschem.2019.108439>
4. C. E. Okafor, U. C. Okonkwo, and I. P. Okokpujie, Trends in reinforced composite design for ionizing radiation shielding applications: a review. *J Mater Sci*. **56**(20),11631(2021), <https://doi.org/10.1007/s10853-021-06037-3>

5. A. S. Ouda, Development of high-performance heavy density concrete using different aggregates for gamma-ray shielding. *Progress in Nuclear Energy*. **79**,48(2015), <https://doi.org/10.1016/j.pnucene.2014.11.009>
6. S. Barbhuiya, B. B. Das, P. Norman, and T. Qureshi, A comprehensive review of radiation shielding concrete: Properties, design, evaluation, and applications. *Structural Concrete*. **26**(2),1809 (2025), <https://doi.org/10.1002/suco.202400519>.
7. M. Erdem, O. Baykara, M. Doğru, and F. Kuluöztürk, A novel shielding material prepared from solid waste containing lead for gamma ray. *Radiation Physics and Chemistry*. **79**(9),917(2010), <https://doi.org/10.1016/j.radphyschem.2010.04.009>.
8. G. L. Stukenbroeker, C. F. Bonilla, and R. W. Peterson, The use of lead as a shielding material. *Nuclear Engineering and Design*. **13**(1),3(1970), [https://doi.org/10.1016/0029-5493\(70\)90030-0](https://doi.org/10.1016/0029-5493(70)90030-0)
9. N. Ahmad, M. I. Idris, A. Hussin, J. Abdul Karim, N. Azreen, and R. Zainon, Enhancing shielding efficiency of ordinary and barite concrete in radiation shielding utilizations. *Sci Rep*. **14**(1),26029(2024), <https://doi.org/10.1038/s41598-024-76402-0>.
10. H. Needleman, Lead poisoning. *Annu. Rev. Med.* **55**(1), 209(2004), <https://doi.org/10.1146/annurev.med.55.091902.103653>.
11. A. H. Alsaab and S. Zeghib, Study of prepared lead-free polymer nanocomposites for X-and gamma-ray shielding in healthcare applications. *Polymers*. **15**(9), 2142(2023), <https://doi.org/doi.org/10.3390/polym15092142>.
12. S. Mortazavi, J. J. Bevelacqua, P. Rafiepour, S. Sina, J. Moradgholi, A. Mortazavi, and J. S. Welsh, Lead-free, multilayered, and nanosized radiation shields in medical applications, industrial, and space research, *Advanced Radiation Shielding Materials*.305(2024),<https://doi.org/10.1016/B978-0-323-95387-0.00006-6>.
13. Z. Khattari, N. A. Alsaif, M. Shams, R. Elsad, and Y. Rammah, Development of materials from natural clay minerals and magnesia useful for radiation-shielding applications. *Silicon*. **15**(11),4897(2023), <https://doi.org/10.1007/s12633-023-02400-y>.
14. M. J. Catenacci, H. R. Luckarift, R. J. Friedman, A. Male, and J. R. Owens, Effect of fly ash composition and component quantities on the gamma radiation shielding properties of geopolymer. *Progress in Nuclear Energy*, **140**, 103889 (2021), <https://doi.org/10.1016/j.pnucene.2021.103889>.
15. F. R. P. Plando, M. B. Z. Gili, and J. T. Maquiling, Microstructural characterizations and radiation shielding quantities of rice husk ash-based self-compacting concrete and its precursors. *Radiation Physics and Chemistry*. **208**,110916(2023), <http://dx.doi.org/10.2139/ssrn.4361294>.
16. U. Rilwan, M. Abdulazeez, I. Maina, O. Olasoji, A. El-Taher, I. Adeshina, and M. Sayyed, Sustainable gamma radiation shielding: coconut shell ash modified concrete for radiation protection applications. *Journal of Radiation and Nuclear Applications*. **10**(1), 33(2025), <https://doi.org/10.18576/jrna/100106>.
17. M. W. N. Hin, P. Ramadhansyah, and K. Masri, *Palm Oil Fuel Ash, Garnet Waste and Sawdust as Modified Asphalt Mixture: A Critical Review*, in *IOP Conference Series: Earth and Environmental Science*. 2024, IOP Publishing. pp. 012004. <https://doi.org/10.1088/1755-1315/1296/1/012004>.
18. E. T. Akinlabi, K. Anane-Fenin, and D. R. Akwada, Bamboo. *The Multipurpose Plant*. **268**,(2017), <https://doi.org/10.1007/978-3-319-56808-9>.
19. W. Liese and T. K. H. Tang, *Preservation and drying of bamboo*, in *Bamboo: the plant and its uses*. 2015, Springer. p. 257, https://doi.org/10.1007/978-3-319-14133-6_9.
20. N. Jiyas, I. Sasidharan, K. Bindu Kumar, B. Gopakumar, M. Dan, and B. Sabulal, Mechanical superiority of Pseudoxytenanthera bamboo for sustainable engineering solutions. *Sci Rep*. **13**(1),18169 (2023), <https://doi.org/10.1038/s41598-023-45523-3>.
21. T. G. Ayoola, O. A. Olufemi, and O. K. Adesola, Mechanical characteristics of Biomaterial Particles Reinforced Epoxy Resin Composites for Automobile Accessories. *Ann. Sci. Technol.* **7**,9(2022), <https://doi.org/10.2478/ast-2022-0002>
22. I. O. Olarinoye, M. T. Kolo, I. W. Fawole, and S. O. Salihu, Characterising metal slag-based geopolymer concrete for radiation shielding application. *Confluence University Journal of Science and Technology*. **2**(2), 2025, <https://doi.org/10.5455/CUJOSTECH.250409>.
23. M. Ali, M. Eisa, A. El Faki, A. Hamed, and A. Beineen, Evaluation of efficiency and performances of building materials used in Sudan combined with lead as the gamma ray shieldings. *Intl J Trend Sci Res Dev (IJTSRD)*. **3**(4), 2456(2019), <https://doi.org/10.31142/ijtsrd23924>.
24. C. G. H. Murillo, L. A. E. Velasco, D. J. Acevedo, H. R. V. Carrillo, D. M. del Rio, and H. A. de León Martínez, Concrete blocks, ionizing radiation shielding characteristics. (2021).
25. S. Özen, C. Şengül, T. Erenoglu, Ü. Çolak, I. A. Reyhancan, and M. A. Taşdemir, Properties of heavyweight concrete for structural and radiation shielding purposes. *Arabian Journal for Science and Engineering*. **41**(4),1573(2016). <https://doi.org/10.1007/s13369-015-1868-6>.
26. J. Han, Z. Xi, R. Yu, J. Guan, Y. Lv, and G. Li, Preparation and comprehensive properties of a high-radiation-shielding UHPC by using magnetite fine aggregate. *Materials*. **15**(3), 978(2022), <https://doi.org/doi.org/10.3390/ma15030978>.

27. N. Jaha, G. S. Islam, M. F. Kabir, M. U. Khandaker, F.-U.-Z. Chowdhury, and A. S. I. Bhuiyan, Ionizing radiation shielding efficacy of common mortar and concrete used in Bangladeshi dwellings. *Case Studies in Construction Materials*. 17, e01547(2022), <https://doi.org/10.1016/j.cscm.2022.e01547>.

أداء الحماية من أشعة جاما لمركبات الملاط الأسمنتي والخيزران الشائع

لطيف مصطفى¹ وإبراهيم دبلبو فاولي² وإليسانمي أ. أوجو¹ وجانيو أ. تيكاويو³ وعبد الله يو يو أوتشيني²
و مورينكيجي دبلبو أتاندا¹ وبيتر أو إيجبايلو¹
قسم العلوم الفيزيائية، جامعة الحكمة، إيلورين، ولاية كوارا، نيجيريا
قسم الفيزياء، جامعة ماينوغوري، ماينوغوري، ولاية بورنو، نيجيريا
قسم الهندسة الميكانيكية، جامعة أوبافيمي أولو، إيلي إيفي، ولاية أوسون، نيجيريا

الخلاصة

تُعرف كتل الرصاص والخرسانة بقدرتها على الحماية من الإشعاع المؤين، إلا أن استخدامها محدود بسبب كثافتها العالية وسميتها ومخاوفها البيئية. تبحث هذه الدراسة إمكانية استخدام مركبات الملاط المصنوعة من مسحوق الخيزران (*Bambusa vulgaris*) كبديل للحماية من أشعة غاما. تم تحضير مزيج من مسحوق الخيزران والرمل والأسمنت بنسب وزنية مختلفة (0-80، 0-80، 14.29-25.0% وزناً على التوالي) لإنتاج مركبات ثنائية وثلاثية. تم تحديد التركيب العنصري لمسحوق الخيزران باستخدام تقنية التألق بالأشعة السينية (XRF)، بينما تم تحديد معاملات امتصاص الإشعاع للعينات باستخدام كاشف وميض من يوديد الصوديوم المنشط بالتاليوم (NaI(Tl)) ومصدر أشعة غاما من السيزيوم-137 (662 كيلو إلكترون فولت). تم تحديد معايير الحماية الرئيسية، بما في ذلك معاملات التوهين الخطي والكتلي (LACs و MACs)، وطبقة نصف القيمة (HVL)، وطبقات عُشر القيمة (TVL)، ومتوسط المسار الحر (MFP)، والإجهاد الانضغاطي. أظهر المركب الذي يحتوي على 57.14% من الخيزران، و28.57% من الرمل، و14.29% من الأسمنت، أفضل خصائص التوهين، حيث بلغت قيم LAC و MAC و HVL و TVL و MFP والإجهاد 1.015 سم⁻¹، و1.067 سم²/غ، و0.683 سم، و2.269 سم، و0.985 سم، و0.620 كيلو باسكال على التوالي. يتميز هذا المركب بقدرته على امتصاص الإشعاع مع انخفاض الإجهاد الميكانيكي. لذا، يمكن دراسة استخدام الملاط المصنوع من الخيزران في التطبيقات التي تتطلب الحماية من أشعة غاما.

الكلمات المفتاحية: الخيزران، أشعة جاما، الهاون، التوهين، الحماية.